J Mol Model (2013) 19:1311–1318
DOI 10.1007/s00894-012-1685-8

ORIGINAL PAPER

# Effect of superalkali substituents on the strengths and properties of hydrogen and halogen bonds

**Wenkai Tian · Xin Huang · Qingzhong Li · Wenzuo Li · Jianbo Cheng · Baoan Gong**

Received: 8 October 2012 / Accepted: 7 November 2012 / Published online: 24 November 2012


**Abstract** Quantum chemical calculations have been performed for the complexes $Li_3OCCX$–Y (X=Cl, Br, H; Y= $NH_3$, $H_2O$, $H_2S$) and $Li_3OCN$–X′Y′ (X′Y′=ClF, BrCl, BrF, HF) to study the role of superalkalis in hydrogen and halogen bonds. The results show that the presence of an $Li_3O$ cluster in a Lewis acid weakens its acidity, while its presence in a Lewis base enhances its basicity. Furthermore, the latter effect is more prominent than the former one, and the presence of an $Na_3O$ cluster causes an even greater effect than $Li_3O$. The strengths of hydrogen and halogen bonds were analyzed using molecular electrostatic potentials. The contributions of superalkalis to the strength of hydrogen and halogen bonds were elucidated by analyzing differences in electron density.

**Keywords** Superalkalis · Hydrogen bond · Halogen bond · Electrostatic potentials · Electron density difference

## Introduction

Understanding and utilizing noncovalent interactions are becoming increasing important tasks in modern chemistry, since they play an important role in chemical and biological processes, including molecular recognition and sensors [1–3], crystal engineering [4–6], and enzymatic mechanisms [7–9]. Hydrogen and halogen bonds are two important noncovalent interactions. The former is still a hot research topic in these fields, even though there have been many studies of hydrogen bonds, while the latter has attracted considerable attention in recent years [10–14]. Both types of interactions have similarities in terms of structures and properties, in which the interaction direction and strength are the two main factors to consider when these types of interactions are applied in the fields mentioned above. Halogen bonding is more linear than hydrogen bonding [15], although both of them are electrostatically driven noncovalent interactions. It has been demonstrated that the interaction energy of halogen bonding is correlated with the positive electrostatic potential (σ-hole) on the covalently bonded halogen [16–18]. The existence of σ-holes on the surfaces of covalently bonded group V and VI atoms has also been confirmed [19]. Very recently, Politzer et al. presented a perspective on halogen bonding and other σ-hole interactions [20].

It is known that the strengths of hydrogen and halogen bonds are mainly related to the atoms and groups that directly participate in the interactions. Stronger interactions correspond a more acidic proton or halogen atom and a stronger Lewis base. In addition, their strengths can be regulated through substitution [21–28]. We compared the strengths of single-electron halogen bonds in $CH_3$–BrH, $CH_3CH_2$–BrH, $(CH_3)_2CH$–BrH, and $(CH_3)_3C$–BrH complexes, and found that the methyl group in the Lewis base enhances the halogen bond [26]. An unexpected enhancement of halogen bond strength by the methyl groups in dimethyl sulfide has also been reported [27]. Bauzá et al. [28] performed a comprehensive ab initio study of substituent effects in halogen-bonded complexes comprising aromatic donors and acceptors. Interestingly, the effect of the substituent on the interaction energy is similar for both

W. Tian · Q. Li (✉) · W. Li · J. Cheng
The Laboratory of Theoretical and Computational Chemistry, School of Chemistry and Chemical Engineering, Yantai University, Yantai 264005, People's Republic of China
e-mail: liqingzhong1990@sina.com

X. Huang
Institute of Plant Quarantine, Chinese Academy of Inspection and Quarantine, Beijing 100029, People's Republic of China

B. Gong
Yantai Nanshan University, Yantai 264005, People's Republic of China

hydrogen bonds and halogen bonds. However, an unexpected trend was found for the substituents in halogen-bonded complexes of $CX_3I$ (X=F, Cl, Br, I) with two typical Lewis bases (chloride and trimethylamine) [29]. The halogen bond strength of a compound C–I does not necessarily increase as the electronegativity of the (carbon-based) group X increases.

Superalkalis are molecules with ionization potentials that are lower than those of alkali atoms (5.4–3.9 eV) [30]. Many stable superalkalis have been identified using experimental and theoretical methods [31]. For example, alkali oxides of composition $X_3O$ (X=Li, Na, K) are regarded as superalkalis [32]. It has been demonstrated that superalkalis can mimic the chemical behavior of atoms in the periodic table [33].

In the work described in this paper, we focused on the effect of superalkali substituents on the strengths of hydrogen and halogen bonds. Considering that superatoms are potential building blocks for the assembly of novel and nanostructured materials [34], the application of superalkali substitutents in supermolecular chemistry is of great interest to us.

In this paper, the complexes $Li_3OCCX–Y$ (X=Cl, Br, H; Y=$NH_3$, $H_2O$, $H_2S$) and $Li_3OCN–X'Y'$ (X′Y′=ClF, BrCl, BrF, HF) were studied by performing quantum chemical calculations of them. For comparison, the counterparts HCCX–Y and HCN–X′Y′ were also been studied. In addition, the complexes $Na_3OCCBr–NH_3$ and $Na_3OCN–BrF$ were also considered. The main aim of this work was to determine the role played by superalkalis in hydrogen and halogen bonds. The strengths of hydrogen and halogen bonds were evaluated using molecular electrostatic potentials, and the contributions of superalkalis in both types of complexes were analyzed via differences in electron density.

## Theoretical methods

All calculations were performed with the program Gaussian 09 [35]. The structures of the complexes and their monomers were first optimized at the MP2/aug-cc-pVTZ level and then frequency calculations were performed at the same level to confirm the nature of the stationary points. The interaction energy was calculated as the difference between the energy of the complex and the sum of the energies of the respective monomers. The basis set superposition error (BSSE) was removed from the interaction energy using the counterpoise method of Boys and Bernardi [36]. Electrostatic potentials on 0.001 electrons $Bohr^{-3}$ isodensity surfaces were calculated at the MP2/aug-cc-pVTZ level using the program Wave Function Analysis—Surface Analysis Suite (WFA-SAS) [37]. The wavefunctions obtained at the MP2/aug-cc-pVTZ level were employed to determine electron density differences using the program Multiwfn [38], which were then visualized and plotted with the program GaussView 5.0.

## Results and discussion

### Geometries and frequency shifts

The optimized structures of the complexes $Li_3OCCX–Y$ (X=Cl, Br, H; Y=$NH_3$, $H_2O$, $H_2S$) and $Li_3OCN–X'Y'$ (X′Y′=ClF, BrCl, BrF, HF) are shown in Figs. 1 and 2, respectively. The $NH_3$ complexes and the $Li_3OCN–X'Y'$ complexes show $C_{3,v}$ symmetry, while the $H_2O$ and $H_2S$ complexes display $C_s$ symmetry. The geometrical parameters for the $Li_3OCCX–Y$

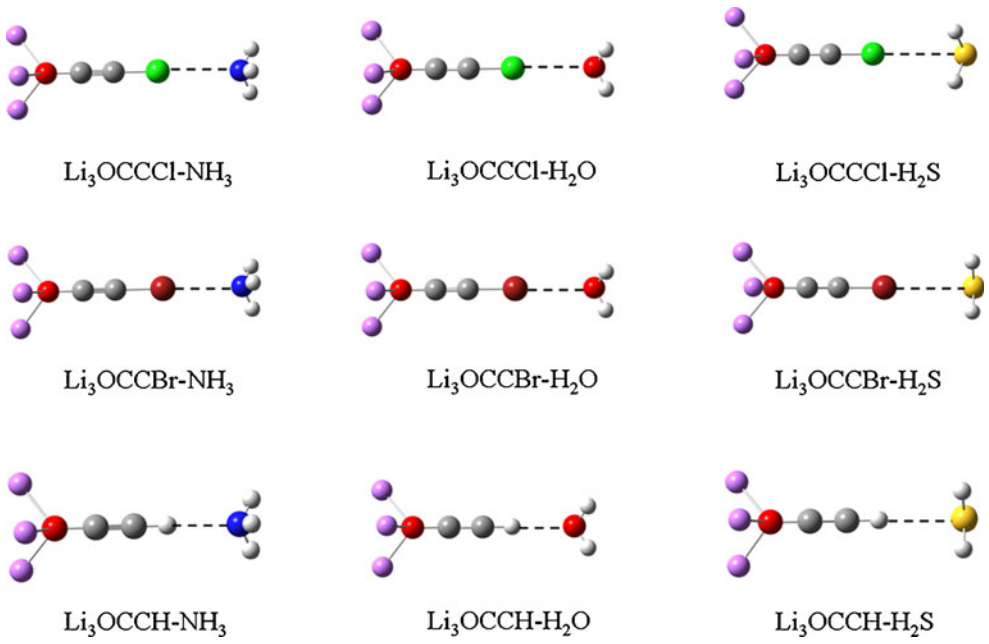


**Fig. 1** Optimized structures of $Li_3OCCX–Y$ (X=Cl, Br, H; Y = $NH_3$, $H_2O$, $H_2S$) complexes

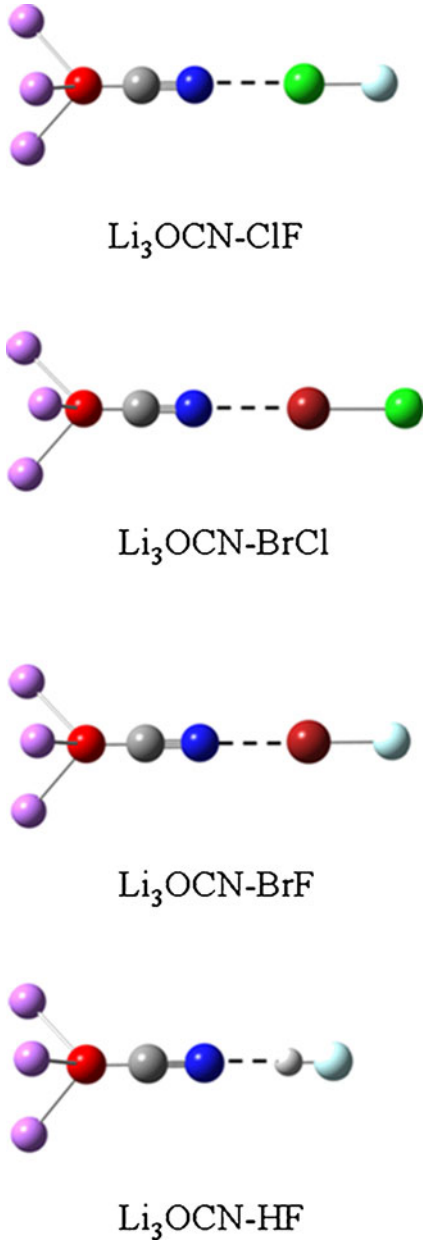


**Fig. 2** Optimized structures of $Li_3OCN$–X′Y′ (X′Y′=ClF, BrCl, BrF, HF) complexes

and $Li_3OCN$–X′Y′ complexes are presented in Tables 1 and 2, respectively. It has been demonstrated that *sp*-hybridized carbon-bound halogen atoms form stronger halogen bonds than $sp^2$- and $sp^3$-hybridized carbon-bound halogen atoms [39]. A similar conclusion was also drawn for hydrogen bonds [40]. Therefore, we selected≡C–X and≡C–H as halogen and proton donors, respectively. The C–X···Y bond angle in the halogen bond is larger than that in the hydrogen bond, which means that the halogen bond has higher directionality than the hydrogen bond. This can be attributed to the effect of the nonbonding valence electrons of the halogen [15]. Evidence for this conclusion is provided by many studies [41–44]. The X···Y–H bond angle in the $H_2S$ complexes is smaller than that in their $H_2O$ counterparts. A similar phenomenon was also observed for other halogen-bonded complexes incorporating O and S atoms [27, 45]. This can be explained by invoking the electrostatic potential maps for $H_2O$ and $H_2S$, as shown in Fig. 3. The most negative electrostatic potential on the surface of the S atom has larger deviation from the molecular plane than that on the surface of the O atom.

The smallest binding distances were obtained for the $Li_3OCCH$ complexes, due to the smaller atomic radius of H. Although the Br atom is larger than Cl, the $Li_3OCCBr$ complexes show smaller binding distances than their $Li_3OCCCl$ counterparts due to stronger interactions. The binding distances in the $Li_3OCCX$ complexes are larger than those in their respective HCCX complexes. However, the binding distance in the $Li_3OCN$ complex is smaller than that in its HCN counterpart. The $Na_3OCCBr\cdots NH_3$ complex presents a larger binding distance than $Li_3OCCBr\cdots NH_3$ does, while the $Na_3OCN\cdots BrF$ complex shows a smaller binding distance than the $Li_3OCN\cdots BrF$ complex.

Upon $Li_3OCCX$–Y complexation, the C–O, C≡C, and C–X bonds are elongated. The C≡C bond shows the least elongation, due to the triple bond. The C–X bond shows more elongation than the C–O bond due to the presence of a direct interaction. Similarly, the formation of the $Li_3OCN$–X′Y′ complex leads to the elongation of the X′–Y′ bond. However, the C≡N bond contracts a little. It was also found that the $Na_3O$ cluster causes a smaller change in the geometry of the $M_3OCCX$–Y complex but a larger change in the geometry of the $M_3OCN$–X′Y′ complex than the $Li_3O$ cluster does.

It is clear from Tables 2 and 3 that a redshift occurs for the stretch vibrations of the C–O, C≡C, and C–X bonds in the $Li_3OCCX$ complex and for the vibration of the X′–Y′ bond in the $Li_3OCN$ complex, while a blueshift is observed for the stretch vibration of the C≡N bond in the $Li_3OCN$ complex upon complexation. These shifts are consistent with the changes in the lengths of these bonds with complexation. The redshifts of the C–Cl and C–Br stretch vibrations vary irregularly with increasing interaction strength, since coupling occurs between the C–X stretch vibration and other bonds. As expected, the redshifts of the C–H and X′–Y′ stretch vibrations reflect the interaction strength.

## Interaction energy

Interaction energy is often used to estimate the strengths of noncovalent interactions. Table 3 presents the interaction energies of these systems, corrected for BSSE. The ratio of BSSE to raw interaction energy is 6~30 % and increases as the interaction in the $Li_3OCCX$–Y system weakens. The BSSE has a greater effect on the halogen bond in the $Li_3OCN$–X′Y′ system. Table 4 shows that the interaction

**Table 1** Binding distances ($R$, in Å) as well as changes in bond lengths ($\Delta r$, in Å) and bond angles ($\theta$, in degrees) in $Li_3OCCX$–Y (X=Cl, Br, H; Y= $NH_3$, $H_2O$, $H_2S$) and $Na_3OCCBr$–$NH_3$ complexes upon complexation, calculated at the MP2/aug-cc-pVTZ level

| Complexes | $R$ | $\Delta r_{O\text{-}C}$ | $\Delta r_{C\equiv C}$ | $\Delta r_{C\text{-}X}$ | $\theta_{C\text{–}X\cdots Y}$ | $\theta_{X\cdots Y\text{–}H}$ |
|---|---|---|---|---|---|---|
| $Li_3OCCCl\cdots NH_3$ | 3.101(3.055) | 0.004 | 0.001 | 0.003 | 179.4 | 111.2 |
| $Li_3OCCCl\cdots OH_2$ | 3.033(2.962) | 0.003 | 0.000 | 0.002 | 179.8 | 116.5 |
| $Li_3OCCCl\cdots SH_2$ | 3.552(3.510) | 0.001 | 0.000 | 0.002 | 170.3 | 72.8 |
| $Li_3OCCBr\cdots NH_3$ | 2.990(2.966) | 0.004 | 0.001 | 0.010 | 179.9 | 111.7 |
| $Li_3OCCBr\cdots OH_2$ | 2.980(2.933) | 0.003 | 0.000 | 0.005 | 179.6 | 116.2 |
| $Li_3OCCBr\cdots SH_2$ | 3.468(3.444) | 0.001 | 0.001 | 0.005 | 175.0 | 83.3 |
| $Li_3OCCH\cdots NH_3$ | 2.308(2.259) | 0.005 | 0.001 | 0.009 | 179.1 | 111.3 |
| $Li_3OCCH\cdots OH_2$ | 2.241(2.186) | 0.004 | 0.001 | 0.005 | 178.8 | 120.1 |
| $Li_3OCCH\cdots SH_2$ | 2.833(2.795) | 0.002 | 0.001 | 0.003 | 174.1 | 89.9 |
| $Na_3OCCBr\cdots NH_3$ | 3.057(2.966) | 0.004 | 0.001 | 0.008 | 179.9 | 111.5 |

The data in parentheses are from the respective HCCX–Y system

energies in the $Li_3OCCBr$ complexes are more negative than the corresponding energies in the $Li_3OCCCl$ complexes. For example, the interaction energy is −12.50 kJ mol$^{-1}$ for the $Li_3OCCBr$–$NH_3$ complex, while it is −7.38 kJ mol$^{-1}$ for the $Li_3OCCCl$–$NH_3$ complex. A similar result was obtained when $NH_3$ was replaced by $H_2S$ or $H_2O$. The calculated electrostatic potentials (ESPs; Table 5) agree well with the results discussed above. The most positive electrostatic potential on Br in $Li_3OCCBr$ (0.0417 eV) was more positive than that on Cl in $Li_3OCCCl$ (0.0308 eV). This means that electrostatic interactions play an important role in the halogen-bonded complexes [10]. The interaction energies in the $Li_3OCCH$ complexes are larger than those in the $Li_3OCCCl$ complexes but smaller than those in the $Li_3OCCBr$ complexes. However, the most positive electrostatic potential on the H atom in $Li_3OCCH$ is larger than those on Cl and Br in $Li_3OCCCl$ and $Li_3OCCBr$, respectively. This can be explained by the fact that halogens are more polarizable than hydrogen. The interaction energies in $Li_3OCN$–X′Y′ complexes become more negative in the order X′Y′=BrCl<ClF<HF<BrF. For the halogen-bonded complexes, the most positive electrostatic potential on the halogen atom is consistent with the interaction energy. The sequence of halogen bond strengths given above is in agreement with the results of previous studies [43, 44]. These results indicate that there is competition between halogen bonding and hydrogen bonding [46–48].

The Lewis bases also affect the strengths of both types of interaction. The interaction strength decreases in the order $NH_3$ >$H_2O$>$H_2S$. These results support the conclusion that $NH_3$ is a stronger Lewis base than $H_2O$ and $H_2S$ [49]. The difference between the interaction energies of the $H_2O$ and $H_2S$ complexes is larger for the hydrogen bonds than for the halogen bonds. The most negative ESP values on the three Lewis bases are also in accord with the results mentioned above.

The interaction energies of the HCCX–Y and HCN–X′Y′ complexes are also listed in Table 4. It is clear that the interaction energy in the $Li_3OCCX$ complex becomes less negative relative to the HCCX complex, while it becomes more negative in the $Li_3OCN$ complex in comparison with the HCN complex. For example, the interaction energy changes from −11.42 kJ mol$^{-1}$ in the HCCBr–$H_2O$ complex to −8.68 kJ mol$^{-1}$ in the $Li_3OCCBr$–$H_2O$ complex, while it changes from −21.69 kJ mol$^{-1}$ in the HCN–ClF complex to −31.41 kJ mol$^{-1}$ in the $Li_3OCN$–ClF complex. This suggests that the presence of the $Li_3O$ cluster in a Lewis acid disfavors the formation of hydrogen and halogen bonds, while its presence in a Lewis base enhances the stability of the hydrogen- and halogen-bonded complexes. Analysis of electrostatic potentials indicates that the presence of the $Li_3O$ cluster reduces the maximum positivity of the electrostatic potential on the Lewis acid atom but increases the maximum negativity of the electrostatic potential on the Lewis base atom. The influence of the $Li_3O$ cluster on the

**Table 2** Binding distances ($R$, in Å) as well as changes in bond lengths ($\Delta r$, in Å) and frequency shifts ($\Delta\nu$, in cm$^{-1}$) in $Li_3OCN$–X′Y′ (X′Y′=ClF, BrCl, BrF, HF) and $Na_3OCN$–BrF complexes upon complexation, calculated at the MP2/aug-cc-pVTZ level

| Complexes | $R$ | $\Delta r_{X'\text{–}Y'}$ | $\Delta r_{C\equiv N}$ | $\Delta\nu_{X'\text{–}Y'}$ | $\Delta\nu_{C\equiv N}$ |
|---|---|---|---|---|---|
| $Li_3OCN\cdots ClF$ | 2.418(2.542) | 0.031 | −0.002 | −73 | 31 |
| $Li_3OCN\cdots BrCl$ | 2.582(2.723) | 0.031 | −0.001 | −33 | 22 |
| $Li_3OCN\cdots BrF$ | 2.354(2.467) | 0.044 | −0.004 | −74 | 50 |
| $Li_3OCN\cdots HF$ | 1.747(1.835) | 0.021 | −0.004 | −452 | 45 |
| $Na_3OCN\cdots BrF$ | 2.274(2.467) | 0.062 | −0.005 | −101 | 71 |

The data in parentheses are from the respective HCN–X′Y′ system

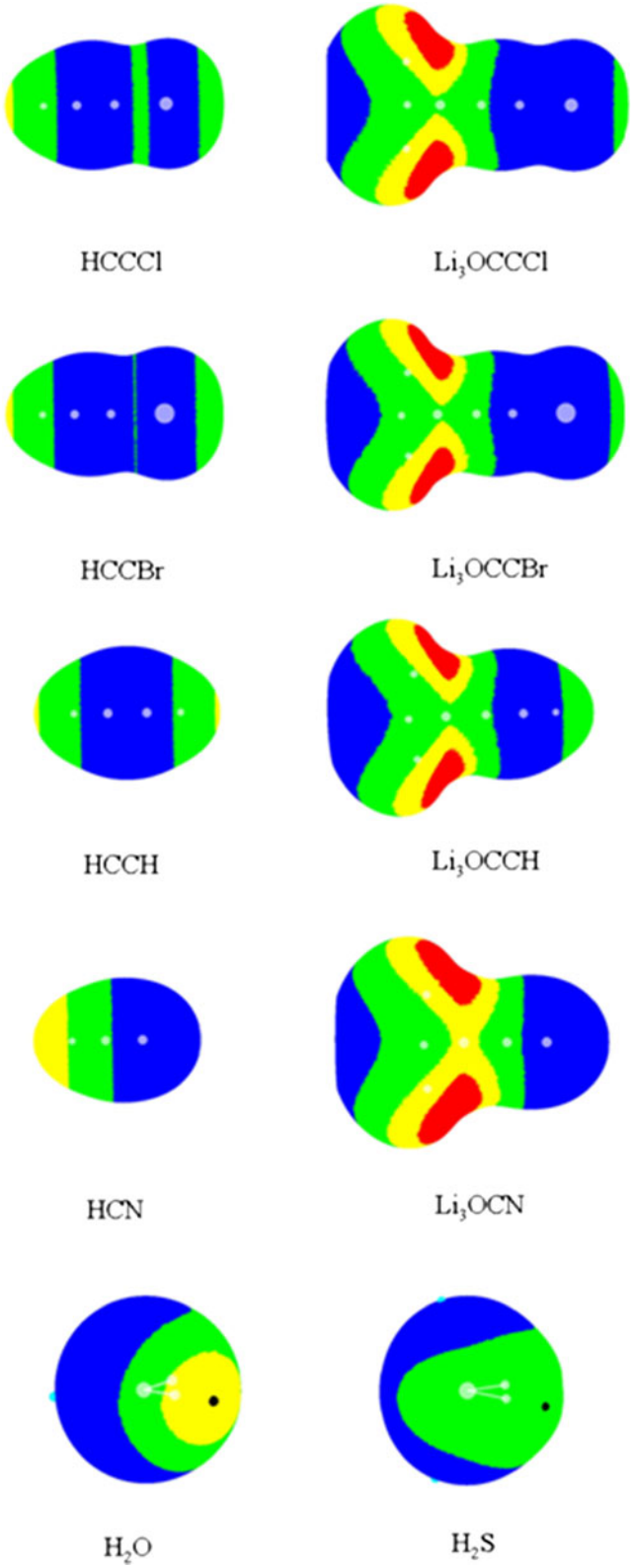


**Fig. 3** The electrostatic potentials on the molecular surfaces of the monomers calculated at the MP2/aug-cc-pVTZ level. *Blue*, less than 0 eV; *green*, between 0 and 0.05 eV; *yellow*, between 0.05 and 0.1 eV; *red*, greater than 0.1 eV

**Table 3** Frequency shifts ($\Delta\nu$, in $cm^{-1}$) in $Li_3OCCX$–Y (X=Cl, Br, H; Y=$NH_3$, $H_2O$, $H_2S$) and $Na_3OCCBr$–$NH_3$ complexes upon complexation, at the MP2/aug-cc-pVTZ level

| Complexes | $\Delta\nu_{O-C}$ | $\Delta\nu_{C\equiv C}$ | $\Delta\nu_{C-X}$ |
|---|---|---|---|
| $Li_3OCCCl\cdots NH_3$ | −10 | −6 | −4 |
| $Li_3OCCCl\cdots OH_2$ | −7 | −4 | −1 |
| $Li_3OCCCl\cdots SH_2$ | −4 | −3 | −38 |
| $Li_3OCCBr\cdots NH_3$ | −12 | −10 | −3 |
| $Li_3OCCBr\cdots OH_2$ | −8 | −6 | 0 |
| $Li_3OCCBr\cdots SH_2$ | −5 | −6 | −3 |
| $Li_3OCCH\cdots NH_3$ | −12 | −18 | −118 |
| $Li_3OCCH\cdots OH_2$ | −8 | −10 | −59 |
| $Li_3OCCH\cdots SH_2$ | −5 | −8 | −44 |
| $Na_3OCCBr\cdots NH_3$ | −13 | −10 | −9 |

interaction strength depends on the nature of the Lewis acid or base. The decrease in the interaction energy caused by the $Li_3O$ cluster in the $Li_3OCCX$–Y complexes follows the order $Li_3OCCBr<Li_3OCCH<Li_3OCCCl$ except in the $H_2S$ system and $H_2S<NH_3<H_2O$ (varying from 14 % to 51 %), whereas the increase in the interaction energy in $Li_3OCN$–X′Y′ complexes caused by the $Li_3O$ cluster follows the order HF< ClF<BrF<BrCl (varying from 42–95 %). Furthermore, the $Li_3O$ cluster has a greater effect on a Lewis base than on a Lewis acid. If the $Li_3O$ cluster is replaced by a $Na_3O$ cluster,

**Table 4** Interaction energy corrected for BSSE ($\Delta E_{CP}$, in $kJmol^{-1}$) in $Li_3OCCX$–Y (X=Cl, Br, H; Y=$NH_3$, $H_2O$, $H_2S$), $Na_3OCCBr$–$NH_3$, $Li_3OCN$–X′Y′ (X′Y′=ClF, BrCl, BrF, HF), and $Na_3OCN$–BrF complexes as well as the percentage (%) change in this parameter relative to the corrected interaction energies of the corresponding unsubstituted systems, calculated at the MP2/aug-cc-pVTZ level

| Complexes | $\Delta E$ | BSSE | $\Delta E_{CP}$ | % |
|---|---|---|---|---|
| $Li_3OCCCl\cdots NH_3$ | −8.34 | 0.96 | −7.38(−10.46) | −0.29 |
| $Li_3OCCCl\cdots OH_2$ | −6.54 | 1.03 | −5.51(−8.21) | −0.33 |
| $Li_3OCCCl\cdots SH_2$ | −6.49 | 1.21 | −5.28(−6.28) | −0.16 |
| $Li_3OCCBr\cdots NH_3$ | −15.57 | 3.07 | −12.50(−15.76) | −0.21 |
| $Li_3OCCBr\cdots OH_2$ | −11.27 | 2.59 | −8.68(−11.42) | −0.24 |
| $Li_3OCCBr\cdots SH_2$ | −10.55 | 2.79 | −7.76(−9.01) | −0.14 |
| $Li_3OCCH\cdots NH_3$ | −12.63 | 1.78 | −10.85(−14.59) | −0.26 |
| $Li_3OCCH\cdots OH_2$ | −10.17 | 1.87 | −8.30(−11.40) | −0.27 |
| $Li_3OCCH\cdots SH_2$ | −7.17 | 1.83 | −5.34(−6.70) | −0.20 |
| $Na_3OCCBr\cdots NH_3$ | −10.56 | 2.77 | −7.79(−15.76) | −0.51 |
| $Li_3OCN\cdots ClF$ | −35.00 | 3.59 | −31.41(−21.69) | 0.45 |
| $Li_3OCN\cdots BrCl$ | −35.53 | 7.45 | −28.08(−18.78) | 0.50 |
| $Li_3OCN\cdots BrF$ | −55.15 | 9.33 | −45.82(−31.09) | 0.47 |
| $Li_3OCN\cdots HF$ | −46.97 | 3.18 | −43.79(−30.74) | 0.42 |
| $Na_3OCN\cdots BrF$ | −70.86 | 10.32 | −60.54(−31.09) | 0.95 |

The data in parentheses are from the respective HCCX–Y and HCN–X′ Y′ systems

**Table 5** The most positive electrostatic potentials ($V_{max}$, in eV) and the most negative electrostatic potentials ($V_{min}$, in eV) on the surfaces of the atoms shown in bold, calculated at the MP2/aug-cc-pVTZ level

| Monomer | $V_{max}$ | Monomer | $V_{min}$ |
|---|---|---|---|
| $Li_3OCC$**Cl** | 0.0308(0.0382) | **N**$H_3$ | −0.0630 |
| $Li_3OCC$**Br** | 0.0417(0.0486) | $H_2$**O** | −0.0568 |
| $Li_3OCC$**H** | 0.0479(0.0572) | $H_2$**S** | −0.0285 |
| $Na_3OCC$**Br** | 0.0243(0.0486) | HC**N** | −0.0535 |
| **Cl**F | 0.0765 | $Li_3OC$**N** | −0.0666 |
| **Br**Cl | 0.0597 | $Na_3OC$**N** | −0.0866 |
| **Br**F | 0.0926 | | |
| **H**F | 0.1193 | | |

The data in parentheses are from the HCCX monomers

this effect is more prominent. In particular, in the $Na_3OCN\cdots BrF$ complex, the interaction energy is −60.54 kJ $mol^{-1}$, which corresponds to strong halogen bonds.

## Electron density difference

To gain insight into the contribution of the $Li_3O$ cluster to Lewis acids and bases, we analyzed the changes in electron density that occurred during the formation of the complexes. It has been demonstrated that total electron density maps are useful for accurately determining electron density shifts [50].

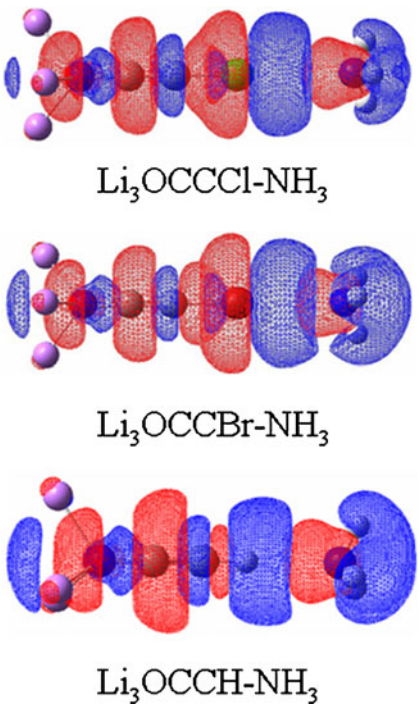


**Fig. 4** Electron density shifts in the indicated $Li_3OCCX–NH_3$ (X=Cl, Br, H) complexes upon the formation of each complex. *Red* regions indicate increased density, *blue* regions indicate decreased density. Contours are shown at the 0.0001 au level

The shifts that occur in the $Li_3OCCX–NH_3$ and $Li_3OCN–X'Y'$ complexes are illustrated in Figs. 4 and 5, respectively. These maps were generated by comparing the electron density in the complex to the sum of the electron densities of the isolated subsystems frozen in the optimized structure of the complex. Red regions indicate increased electron density, while blue regions represent decreased electron density.

As expected, the hydrogen-bonded complexes exhibit a region (blue) of density loss around the bridging proton, while areas (red) of density accumulation are observed for the lone pair of the proton-accepting N as well as along the covalent C–H and F–H bonds. The side of the N atom in $NH_3$ that points away from the center of the molecule suffers a substantial loss of charge, as indicated by the large blue region. The density shifts seen for the halogen bonds are quite similar to those seen for the hydrogen bonds. The red region around the carbon–halogen bond is bigger than that of the carbon–hydrogen bond in the $Li_3OCCX–NH_3$ complex. The density shifts seen in the dihalogen molecule are more complicated than those seen for HF in the $Li_3OCN–X'Y'$ complex.

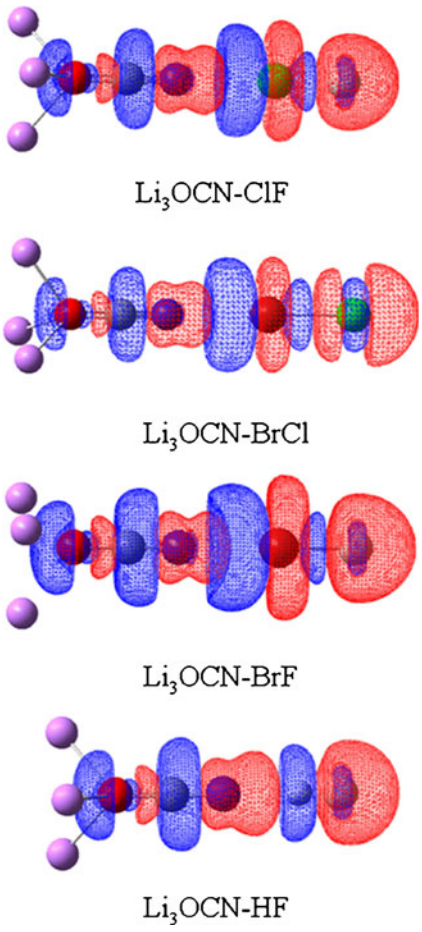


**Fig. 5** Electron density shifts in the indicated $Li_3OCN–X'Y'$ (X′Y′= ClF, BrCl, BrF, HF) complexes upon fthe ormation of each complex. *Red* regions indicate increased density, *blue* regions indicate decreased density. Contours are shown at the 0.0004 au level

Finally, considering the aim of this work, we are most interested in the density shifts seen for the $Li_3O$ clusters in the complexes. It is clear that there is a loss of density around the $Li_3O$ cluster in the $Li_3OCN$ complex and the $Li_3$ in the $Li_3OCCX$ complex, but enhanced density around the O atom in the $Li_3OCCX$ complex. This indicates that the $Li_3O$ cluster is an electron-donating substituent in Lewis acids and bases. The electron donation from the $Li_3O$ cluster in a Lewis acid disfavors the formation of a complex, while this donation is aids complex formation for a Lewis base. The $\pi$ electrons in the $Li_3O$ cluster [51] can be observed in the maps of electrostatic potential shown in Fig. 3. The behavior of the electrons that contribute to the $Li_3O$ cluster is consistent with the presence of these $\pi$ electrons. Also, the blue region of the $Li_3O$ cluster in the $Li_3OCN$ complex is larger than that in the $Li_3OCCX$ complex, which provides support for the conclusion that the $Li_3O$ cluster exerts a greater effect on the former than the latter.

## Conclusions

The complexes $Li_3OCCX$–Y (X=Cl, Br, H; Y=$NH_3$, $H_2O$, $H_2S$) and $Li_3OCN$–X′Y′ (X′Y′=ClF, BrCl, BrF, HF) were investigated at the MP2/aug-cc-pVTZ level of theory. It was found that the presence of the $Li_3O$ cluster in a Lewis acid weakens its hydrogen and halogen bonds, while its presence in a Lewis base strengthens both types of interactions. These effects of the $Li_3O$ cluster are related to the nature of Lewis acids and bases. The presence of the $Li_3O$ cluster in a Lewis acid decreases the most positive electrostatic potential of X, whereas it increases the most negative electrostatic potential of N in a Lewis base. Analysis of electron density differences indicates that the $Li_3O$ cluster is an electron-donating group in Lewis acids and bases, and this electron donation has a negative effect on the stability of the $Li_3OCCX$–Y complex and a positive effect on the stability of the $Li_3OCN$–X′Y′ complex. Furthermore, the presence of a $Na_3O$ cluster exerts an even greater influence on the strengths of hydrogen and halogen bonds than the presence of a $Li_3O$ cluster does.

**Acknowledgments** This work was supported by the Outstanding Youth Natural Science Foundation of Shandong Province (JQ201006) and the Program for New Century Excellent Talents in University.

## References

1. Maffei F, Betti P, Genovese D, Montalti M, Prodi L, Zorzi RD, Geremia S, Dalcanale E (2011) Angew Chem Int Ed 50:4654–4657
2. Chudzinski MG, McClary CA, Taylor MS (2011) J Am Chem Soc 133:10559–10567
3. Caballero A, White NG, Beer PD (2011) Angew Chem Int Ed 50:1845–1848
4. Deriraju GR (2002) Acc Chem Res 35:565–573
5. Kataoka K, Yanagi M, Katagiri T (2011) Cryst Eng Comm 13:6342–6344
6. Weyna DR, Cheney ML, Shan N, Hanna M, Wojtas Ł, Zaworotko MJ (2012) Cryst Eng Comm 14:2377–2380
7. Hanoian P, Sigala PA, Herschlag D, Hammes-Schiffer S (2010) Biochemistry 49:10339–10348
8. Krauta DA, Sigalaa PA, Fennb TD, Herschlaga D (2010) Proc Natl Acad Sci USA 107:1960–1965
9. Hardegger LA, Kuhn B, Spinnler B, Anselm L, Ecabert R, Stihle M, Gsell B, Thoma R, Diez J, Benz J, Plancher JM, Hartmann G, Banner DW, Haap W, Diederich F (2011) Angew Chem Int Ed 50:314–318
10. Politzer P, Murray JS, Clark T (2010) Phys Chem Chem Phys 12:7748–7757
11. Nelyubina YV, Antipin MY, Dunin DS, Kotov VY, Lyssenko KA (2010) Chem Commun 46:5325–5327
12. Li QZ, Li R, Liu ZB, Li WZ, Cheng JB (2011) J Comput Chem 32:3296–3303
13. Zhang Y, Ma N, Wang WZ (2012) Chem Phys Lett 532:27–30
14. Alkorta I, Sanchez-Sanz G, Elguero J (2012) J Phys Chem A 116:2300–2308
15. Shields ZP, Murray JS, Politzer P (2010) Int J Quantum Chem 110:2823–2832
16. Riley KE, Murray JS, Politzer P, Concha MC, Hobza P (2009) J Chem Theory Comput 5:155–163
17. Riley KE, Murray JS, Fanfrlík J, Řezáč J, Solá RJ, Concha MC, Ramos FM, Politzer P (2012) J Mol Model. doi:10.1007/s00894-012-1428-x
18. Bundhun A, Ramasami P, Murray JS, Politzer P (2012) J Mol Model. doi:10.1007/s00894-012-1571-4
19. Murray JS, Lane P, Politzer P (2009) J Mol Model 15:723–729
20. Politzer P, Riley KE, Bulat FA, Murray JS (2012) Comput Theor Chem 998:2–8
21. Alkorta I, Rozas I, Elguero J (2000) J Fluorine Chem 101:233–238
22. Nagaraju M, Sastry GN (2011) J Mol Model 17:1801–1816
23. Li QZ, Ma SM, Liu XF, Li WZ, Cheng JB (2012) J Chem Phys 137(8):084314
24. Ishikawa R, Ono A, Kainosho M (2003) Nucleic Acids Res Suppl 3:57–58
25. Riley KE, Murray JS, Fanfrlík J, Rezáč J, Solá RJ, Concha MC, Ramos FM, Politzer P (2011) J Mol Model 17:3309–3318
26. Li QZ, An XL, Gong BA, Cheng JB (2008) J Mol Struct: THEOCHEM 866:11–14
27. Li QZ, Jing B, Liu ZB, Li WZ, Cheng JB, Gong BA, Sun JZ (2010) J Chem Phys 133:114303
28. Bauzá A, Quiñonero D, Frontera A, Deyà PM (2011) Phys Chem Chem Phys 13:20371–20379
29. Huber SM, Jimenez-Izal E, Ugalde JM, Infante I (2012) Chem Commun 48:7708–7710
30. Gutsev GL, Boldyrev AI (1985) Adv Chem Phys 61:169–221
31. Rehm E, Boldyrev AI, Schleyer PR (1992) Inorg Chem 31:4834–4842
32. Dao PD, Peterson KI, Castleman AW Jr (1984) J Chem Phys 80:563–564
33. Bergeron DE, Castleman AW Jr, Morisato T, Khanna SN (2004) Science 304:84–87
34. Koirala P, Willis M, Kiran B, Kandalam AK, Jena P (2010) J Phys Chem C 114:16018–16024
35. Frisch MJ, Trucks GW, Schlegel HB, Scuseria GE, Robb MA, Cheeseman JR, Montgomery JA Jr, Vreven T, Kudin KN, Burant JC, Millam JM, Iyengar SS, Tomasi J, Barone V, Mennucci B, Cossi M, Scalmani G, Rega N, Petersson GA, Nakatsuji H, Hada M, Ehara M, Toyota K, Fukuda R, Hasegawa J, Ishida M, Nakajima T, Honda Y, Kitao O, Nakai H, Klene M, Li X, Knox JE, Hratchian HP, Cross JB, Adamo C, Jaramillo J, Gomperts R, Stratmann RE, Yazyev O, Austin AJ, Cammi R, Pomelli C, Ochterski JW, Ayala PY,

Morokuma K, Voth GA, Salvador P, Dannenberg JJ, ZakrzewskiVG DS, Daniels AD, Strain MC, Farkas O, Malick DK, Rabuck AD, Raghavachari K, Foresman JB, Ortiz JV, Cui Q, Baboul AG, Clifford S, Cioslowski J, Stefanov BB, Liu G, Liashenko A, Piskorz P, Komaromi I, Martin RL, Fox DJ, Keith T, Al-Laham MA, Peng CY, Nanayakkara A, Challacombe M, Gill PMW, Johnson B, Chen W, Wong MW, Gonzalez C, Pittsburgh PA, Pople JA (2009) Gaussian 09, revision A02. Gaussian Inc, Wallingford
36. Boys SF, Bernardi F (1970) Mol Phys 19:553–566
37. Bulat FA, Toro-Labbé A, Brinck T, Murray JS, Politzer P (2010) J Mol Model 16:1679–1691
38. Lu T, Chen FW (2012) J Comput Chem 33:580–592
39. Zou JW, Jiang YJ, Guo M, Hu GX, Zhang B, Liu HC, Yu QS (2005) Chem Eur J 11:740–751
40. Scheiner S, Grabowski SJ, Kar T (2001) J Phys Chem A 105:10607–10612
41. Tsuzuki S, Wakisaka A, Ono T, Sonoda T (2012) Chemistry 18:951–960
42. Mukai T, Nishikawa K (2010) X-Ray Struct Anal 26:31–32
43. Legon AC (1999) Angew Chem Int Ed 38:2686–2714
44. Li QZ, Li R, Zhou ZJ, Li WZ, Cheng JB (2012) J Chem Phys 136:014302
45. Ban QF, Li R, Li QZ, Li WZ, Cheng JB (2012) Comput Theor Chem 991:88–92
46. Alkorta I, Blanco F, Solimannejad M, Elguero J (2008) J Phys Chem A 112:10856–10863
47. Politzer P, Murray JS, Lane P (2007) Int J Quant Chem 107:3046–3052
48. Li QZ, Xu XS, Liu T, Jing B, Li WZ, Cheng JB, Gong BA, Sun JZ (2010) Phys Chem Chem Phys 12:6837–6843
49. Legon AC (2008) Struct Bond 126:17–64
50. Scheiner S, Kar T (2002) J Phys Chem A 106:1784–1789
51. Wang YF, Chen W, Yu GT, Li ZR, Sun CC (2010) Int J Quant Chem 110:1953–1963